Available online at www.sciencedirect.com
ScienceDirect
Journal of the European Ceramic Society 28 (2008) 1049–1056
www.elsevier.com/locate/jeurceramsoc

"Snow flake" structures in silicon nitride ceramics – Reasons for large scale optical inhomogeneities

Mathias Herrmann *, Ingrid Schulz, Axel Bales, Kerstin Sempf, Soeren Hoehn

Fraunhofer Institute for Ceramic Technologies and Systems, Winterbergstrasse 28, D-01277, Dresden, Germany

Available online 30 October 2007

Abstract

Large scale optical inhomogeneities were analysed in different Si_3N_4 ceramics containing different additive ratios and densified by hot pressing, gas pressure sintering and spark plasma sintering.

In all analysed materials showing these optical inhomogeneities ("snow flakes") non-filled triple junctions were locally found which could be correlated with the "snow flake" structure. The internal tensile stress in the amorphous grain boundary phase is the most likely reason for this phenomenon. These stresses are caused by thermal mismatch between the grain boundary phase and the Si_3N_4 skeleton, or the volume change during crystallisation of the grain boundary phase.

Keywords: Sintering; Silicon nitride; Microstructure

1. Introduction

Because of the continuously increasing requirements on ceramic components, the demands on manufacturing technologies and materials are also growing. Defects in submicrocrystalline and nanocrystalline areas play an increasing role in abrasive application such as ball bearings and cutting tools.[1]

In many liquid phase sintered non-oxide materials local optical inhomogeneities with dimensions in the millimeter range (so called "snow flake" structures) were found which cannot be correlated with inhomogeneities of the composition or of the structure in the mm range. The reasons for these optical inhomogeneities have not been completely understood yet. Particularly with silicon nitride ceramic ball bearings, where local mechanical loads occur, such inhomogeneities are to be regarded as potential source for pitting formations, because the materials in this areas show a different microhardness and unequal polishing behaviour.[2] The "snow flake" structures occur in HPSN, SSN, GPSN and SRBSN irrespective of the manufacturing method. There are different reasons mentioned in the literature:

- micropores due to local uncompleted sintering[3]
- microcracks due to crystallisation of β-$Y_2Si_2O_7$[4]
- locally non-uniform crystallisation [2] resulting in local differences in the refractive indexes.

In an unpublished report[5] about ultrasonic analysis, an increased back scattered ultrasonic signal for Si_3N_4 materials with "snow flake" structures was observed as compared to materials without "snow flake "structures. In this investigation the ultrasonic signals being reflected between the front and back side of the plates (8 mm thickness) were analysed. (The sample was in a water bath, and the ultrasonic frequency was 80 MHz).

This indicates local fluctuations of the Young's modulus or density (Fig. 1). The aim of this paper is to summarise some systematic studies concerning the "snow flake" structure of Si_3N_4 materials.

2. Experimental

Series of Si_3N_4 ceramics with a systematically varied ratio of sintering additives were produced using α-Si_3N_4 powder (UBE SN-E10), Al_2O_3 (AKP50), and Y_2O_3 (grade fine, HCST), Table 1. The ceramics were prepared by mixing the raw powders in isopropanol in a planetary ball mill for 6 h. The suspensions were dried in a rotavap and granulated using a 400 μm sieve. Samples of about 100 g (20 mm × 20 mm × 70 mm) were formed by cold isostatic pressing (250 MPa). Afterwards, the organic binder was removed by heat treatment in air up to 550 °C.

* Corresponding author. Tel.: +49 351 25 53 527; fax: +49 351 25 53 600.
E-mail address: Mathias.Herrmann@ikts.fraunhofer.de (M. Herrmann).

0955-2219/$ – see front matter © 2007 Elsevier Ltd. All rights reserved.
doi:10.1016/j.jeurceramsoc.2007.09.022

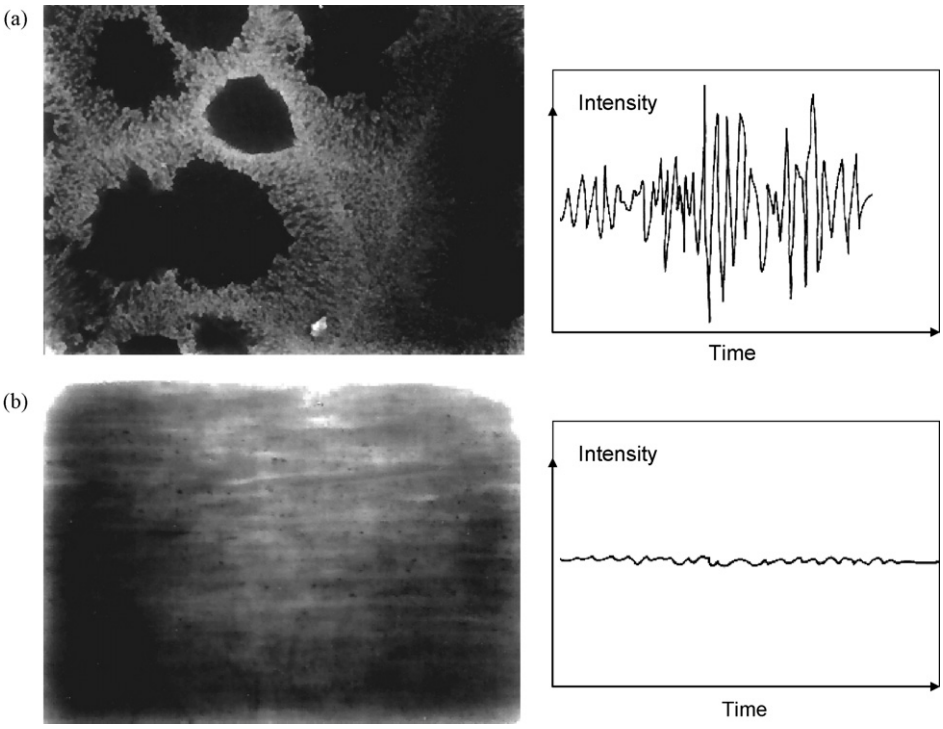

Fig. 1. Dark field image of a sample with "snow flake" structure (a) and without "snow flake" structure (b) and corresponding backscattered ultrasonic signals[5].

Table 1
Composition, density and weight loss during sintering of the materials

Material	Si_3N_4 (%)	Y_2O_3 (%)	Al_2O_3 (%)	Densification	Density (g/cm^3)	Δm (%)	Strength σ_{4b} (MPa)
8Y 2AlGP	90	8	2	Gas pressure sintering	3.281	0.38	1020 ± 70
6Y 4Al GP	90	6	4		3.246	0.55	1030 ± 60
4Y 6Al GP	90	4	6		3.212	0.71	860 ± 60
8Y 2Al HP	90	8	2	Hot pressing	3.326		
6Y 4Al HP	90	6	4		3.243		
4Y 6Al HP	90	4	6		3.211		

The samples were gas pressure sintered at 1825 °C to a density of >99.5% of the theoretical density. Additionally, the samples were hot pressed at 1800 °C for 60 min in nitrogen. The sample 6Y4Al was additionally densified by SPS at 1750 °C.

The samples were cut and parts of the samples were heat treated at different conditions (Table 2). Additionally, in the sintered samples 6Y4Al the grain boundary phase was leached out to a depth of about 200–500 μm using 1 mol/l HNO_3 at 75 °C. Afterwards, these areas were infiltrated again by an oxynitride glass at 1790 °C for 20 min in N_2 (4 bar). Two compositions of the glasses were used: an Y_2O_3 rich glass (62.5 mol% Y_2O_3, 31.2 mol% SiO_2 and 6.6 mol% Al_2O_3) and a silica rich glass (47.6 mol% Y_2O_3, 47.6 mol% SiO_2 and 4.8 mol% Al_2O_3). The preparation procedure of the glass is described in Ref.[6]

All prepared and heat treated samples were cut and the cross sections were polished either by standard ceramographic polishing or by broad ion beam technique (Baltec RES 101). Two different ion beam techniques were used: ion beam polishing

Table 2
Change of the secondary phases and the "snow flake" structure by heat treatment

Material	As densified		Heat treated at 1450 °C and cooled with 1 K/min		Heat treated at 1750 °C, cooled with 5 °C/min to 1250 °C, 1 °C/min to 1100 °C	
	Phases	Snow flakes	Phases	Snow flakes	Phases	Snow flakes
8Y 2AlGP	α-Y_2SiO_5	Strong Type I	β-Y_2SiO_5	Strong Type I	β-Y_2SiO_5	Strong Type I
6Y 4Al GP	amorphous	Small Type I	δ-$Y_2Si_2O_7$	Small Type I	–	–
4Y 6Al GP	Amorphous	Without	Amorphous	Without	–	–
8Y 2Al HP	α-Y_2SiO_5, δ-$Y_2Si_2O_7$	Intensive Type III	β-Y_2SiO_5, $Y_5(SiO_4)_3N$	Intensive Type III	$Y_5(SiO_4)_3N$	Strong Type I
6Y 4Al HP	Amorphous	Less Type II	δ-$Y_2Si_2O_7$	Less Type I	–	–
4Y 6Al HP	Amorphous	Without	Amorphous	Without	–	–

and ion beam cutting. The details are described in Ref.[7] With the ion beam cutting method a cross section was prepared under an angle of 45° to the surface. The cut depth was approximately 50–100 μm on a length of about 1 mm.

The prepared cross sections were analysed using an optical microscope and a FESEM (Leo 982). The phase composition was determined by XRD (XRD7, GE Inspection, CuKα). Four point bending strength (distance of supports 40/20 mm) was determined for some of the materials (Table 1).

3. Results

3.1. "Snow flake" structures in sintered samples

Figs. 1–3 show examples of dark field images of the materials. The phase composition is given in Table 2. The observed "snow flake" structures can be divided by the shape in three main types (Fig. 2, Table 2). Type I shows aggregated areas with a fine substructure like real snow flakes. Type II is characterised by fine white spots. Type III was observed in hot pressed samples and consists of different structures. The main characteristics are ball-like structures with a less structured centre and a rim of nearly constant thickness and strong radial structure. Between the ball-like structures less pronounced, fine structures were observed (Fig. 2).

The shape of the "snow flakes" form strongly depends on the composition and on the densification technique. Materials with a low Y_2O_3/Al_2O_3 ratio, having amorphous grain boundaries, show less or even no "snow flakes". The "snow flake" structure in the samples containing an Y_2O_3/Al_2O_3 ratio of 8:2 is very different, depending on the densification technique: hot pressed or gas pressure sintered (Fig. 2).

The "snow flake" structure does not change during heat treatment at 1450 °C, but strongly changes after heat treatment at

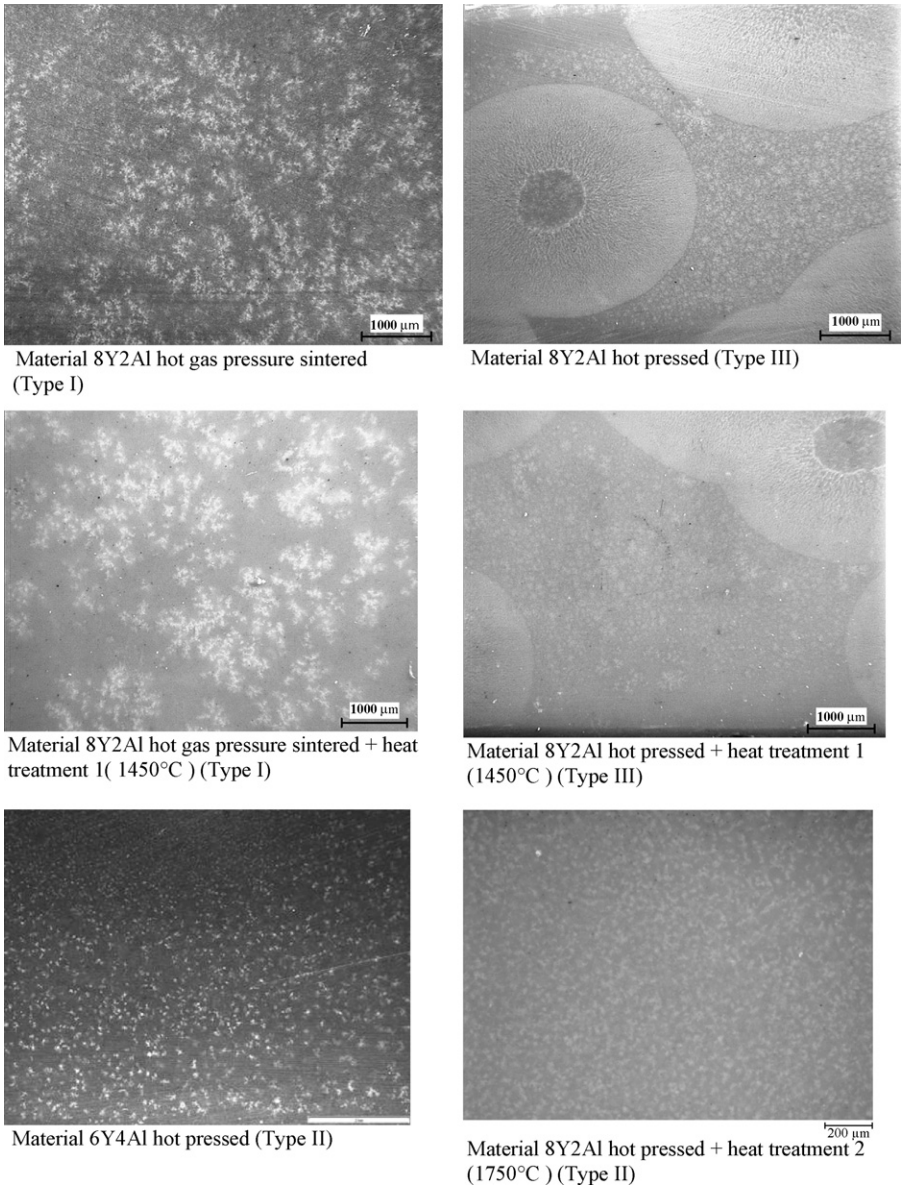

Fig. 2. Dark field images of hot pressed and gas pressure sintered ceramics.

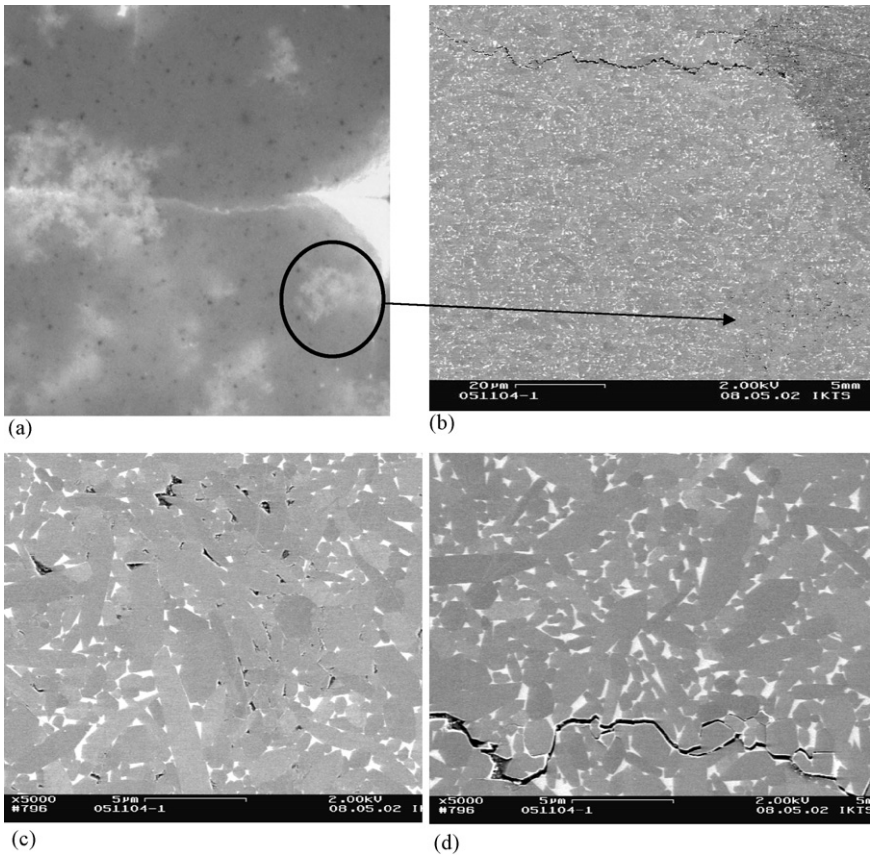

Fig. 3. Dark field image of the material 6Y4AlGPS (with hardness indentation) (a) and corresponding FESEM micrographs produced by ion beam cutting (b, c) area with snow flakes (d) area without snow flakes.

1750 °C or higher (Fig. 2). The SPS densified sample, which shows no "snow flake" structure after densification at all, shows also a "snow flake" structure after additional heat treatment at 1750 °C or 1850 °C which is typical for gas pressure sintered samples under the same conditions.

The detailed analysis of the polished surfaces showed some microporosity in areas with "snow flakes". Some of the samples, therefore, were cut by means the ion beam technique to verify the assumption that microporosity is not caused by the preparation technique. Fig. 3 reveals that the same porosity exists in the ion beam cut samples. Additionally, samples were marked with hardness indentations, and were ion polished. Layers with a thickness of 10–15 μm were removed by ion beam polishing. The advantage of this method is that large areas (1 mm × 1 mm) can be prepared and analysed. Microporosity was also observed under these conditions. This microporosity could be directly correlated with the "snow flake" structure. Summarising these findings it can be stated that in all investigated samples microporosity was observed being similar to that shown in Figs. 3 and 6.

3.2. *"Snow flake" structures in infiltrated samples*

The dark field and bright field images of the glass infiltrated areas are shown in Fig. 4. Dense infiltrated samples could be produced by both glass compositions. In the samples some cracks developed due to the thermal expansion mismatch. In the residual Y_2O_3 rich glass crystalline phases were observed. The much more pronounced "snow flake" structure is clearly visible in the sample infiltrated with Y_2O_3 rich glass (Fig. 4).

Detailed FESEM analyses of the cross section (Fig. 5) showed that the samples are well infiltrated. In large areas the amount of grain boundary phase is higher than in the starting material. This indicates that the glass partially disintegrates the Si_3N_4 skeleton.

At the boundary between the infiltrated and non-infiltrated sample some precipitations of Si were found which are clearly visible as white spots in the bright field images. These precipitations develop due to the interaction of the SiO_2, formed during corrosion, with the Si_3N_4 grains.

4. Discussion

The materials have a bending strength of approximately 1000 MPa (Table 1) despite the fact that the materials have the snow flake structure with dimensions of several 100–1000 μm. These strength values indicate that the defect size of the materials has to be in the range below 50 μm. Therefore, the strength determining defects cannot directly be correlated with the dimension of the "snow flake" structure.

The "snow flake" structure depends strongly on the grain boundary phase composition especially on the crystalline grain boundary phases. Samples with stronger crystallised grain boundary phases showed more pronounced "snow flake" structures. Samples with the same crystalline grain boundary phase

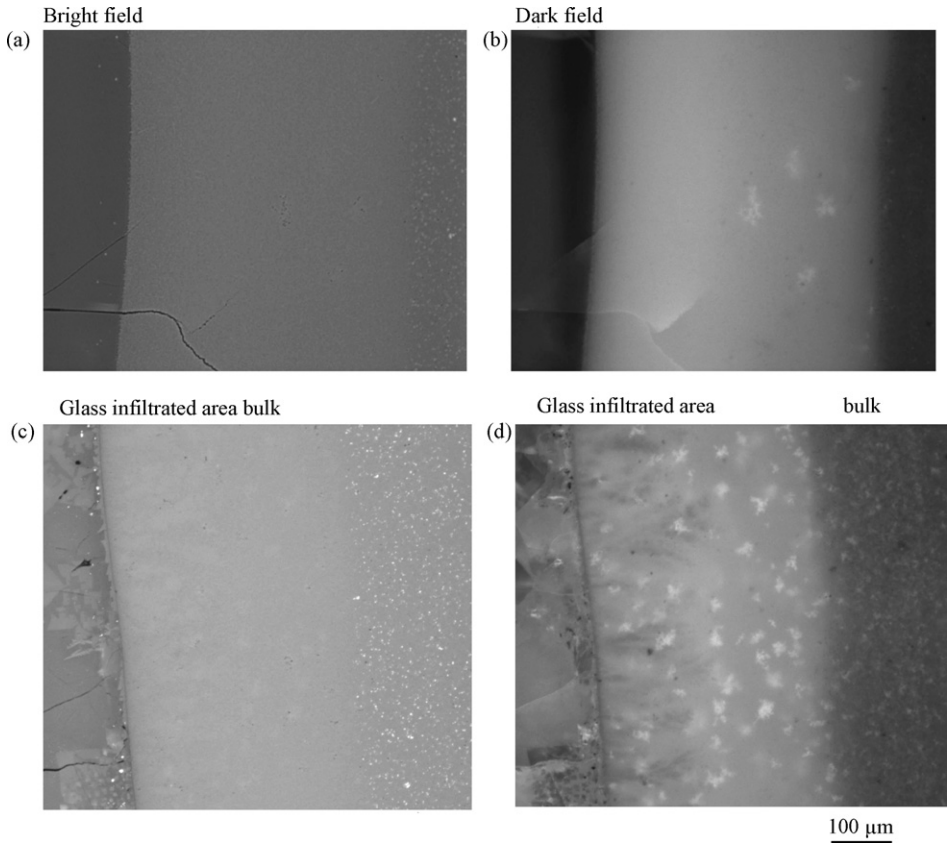

Fig. 4. Bright and dark field micrographs of the infiltrated sample with the glass (47.6 mol% Y_2O_3, 47.6 mol% SiO_2 and 4.8 mol% Al_2O_3) (a, b) and the glass (62.5 mol% Y_2O_3, 31.2 mol% SiO_2 and 6.6 mol% Al_2O_3) (c, d).

have similar "snow flake" structures. This was also found by Keßler.[2] Additionally, the densification influences the "snow flake" structure. Other kinds of "snow flake" structures were observed for hot pressed materials as well as for gas pressure sintered samples. No "snow flake" structures were observed in SPS densified samples and in HIPped materials.[8]

In all investigated samples microporosity was found in areas where "snow flakes" were observed. This porosity was observed irrespective of the preparation methods (ion beam polishing or conventional ceramographic polishing with diamond slurries) of the polished section. The microporosity could directly be correlated with the "snow flake" structure. The pores observed were in the range of less than 1 μm and, therefore, hardly visible in the bright field images. The areas with non-filled triple junctions looked like standard-sintered material in which the grain boundary disappeared after sintering (Figs. 3, 5 and 6).

The detailed analysis of the shape and distribution of the empty triple junctions allow to draw some conclusions concerning the reasons for the "snow flakes".

Before the possible reasons are discussed, it has to be mentioned that all the triple junctions visible in the micrographs are interconnected and form a three dimensional network. This is a consequence of the good wetting behaviour of the oxynitride liquid at high temperatures.[9,10] The fact that the grain boundary phase can be leached out in corrosion experiments proves that these materials form a three dimensional network of the grain boundary.[11]

Bearing this in mind, a redistribution of the grain boundary phase during cooling can even occur in dense materials what can result in the observed clustering of the microporosity.

Different reasons for the observed microporosity can be imagined:

1. Inhomogeneous distribution of sintering additives: signs against this reason can be observed. In materials with a low additive content less or even no "snow flakes" were observed. Investigations of the first sintering phase also show that a redistribution of the additives can take place.[12]

   Additionally, if the triple junctions would be empty during the sintering, the smaller triple junctions have to be filled predominantly. The analysed FESEM micrographs show that small triple junctions can be empty if they are near larger ones (Figs. 3 and 6).
2. Inclusion of gas in the pores, which stabilizes the pores: the data show that "snow flake" structures are independent from the gas pressure (HP or gas pressure sintering). Also in HIPped materials no "snow flakes" were found. If decomposition and a formation of gas phase take place during sintering, larger pores are formed.[13] Solved nitrogen can neither be a reason for the "snow flakes" because they are observed in materials in which residual silicon was detected. This residual silicon would react with the N_2 in the pores, and reduce the gas pressure (Fig. 7). The inward diffusion of nitrogen during the heat treatment process results in the

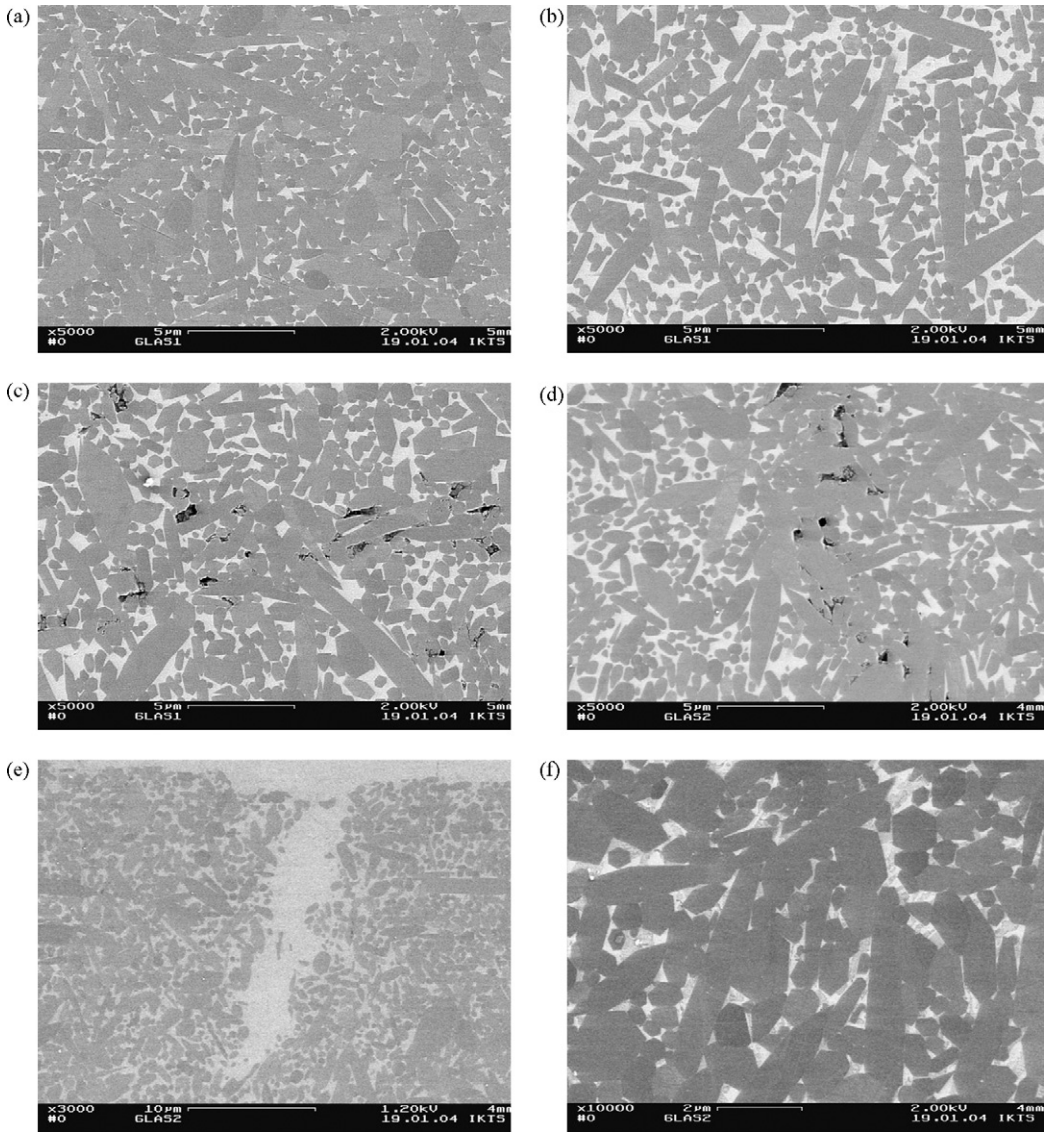

Fig. 5. FESEM micrographs of cross sections of the infiltrated ceramics. (a) Structure before leaching and infiltration. (b and c) Infiltrated with silica rich glass (47.6 mol% Y_2O_3, 47.6 mol% SiO_2 and 4.8 mol% Al_2O_3). (d–f) Infiltrated with Y_2O_3 rich glass (62.5 mol% Y_2O_3, 31.2 mol% SiO_2 and 6.6 mol% Al_2O_3).

low silicon content and the bright colour in the near surface area (Fig. 7). Additionally it has to be mentioned that silicon inclusions can promote the crystallisation of the grain boundaries.

A pore which could be caused by a gas inclusion is shown in Fig. 6b (marked with an arrow). It has a different shape and size in comparison with the observed microporosity. Therefore, this assumption can be ruled out.

3. Bad wetting of the grain boundary phase (at least locally): the glass infiltration experiments show that good wetting occurs. Good wetting is also a precondition for liquid phase sintering. TEM investigations showed good wetting of the Si_3N_4 grains by the glassy phase.[10] So, at least in most of the cases this assumption can be ruled out. However, in LPS SiC materials with Y_2O_3 rich grain boundary phase some signs of segregation due to bad wetting were found.[14] These microstructures were very different from the observed here.

The most likely reason for the formation of the "snow flake" structures are the internal stresses occurring due to the thermal mismatch between the grain boundary phase and Si_3N_4 grains, and the volume change due to crystallisation of the amorphous grain boundary phases.

A simple model for calculating internal stresses[15] gives very low values of internal stresses (20 MPa) for MgO containing glassy phases ($E = 89$ GPa, $\Delta T = 1000\,^{\circ}C$) with a thermal expansion coefficient of ($\alpha = 3.2 \times 10^{-6}\,K^{-1}$) whereas an internal tensile stress of 420 MPa was found for a typical $Y_2O_3/Al_2O_3/SiO_2$ containing grain boundary phase with a thermal expansion coefficient measured on oxynitride glasses ($\alpha = 6.9 \times 10^{-6}\,K^{-1}$). Similar stress levels were determined by Peterson and Tien[16] or using a more complex model.[17,18] The dependence of the thermal expansion coefficient on the SiO_2 content shows that with increasing SiO_2 content in the grain boundary the thermal expansion coefficient drops to the value

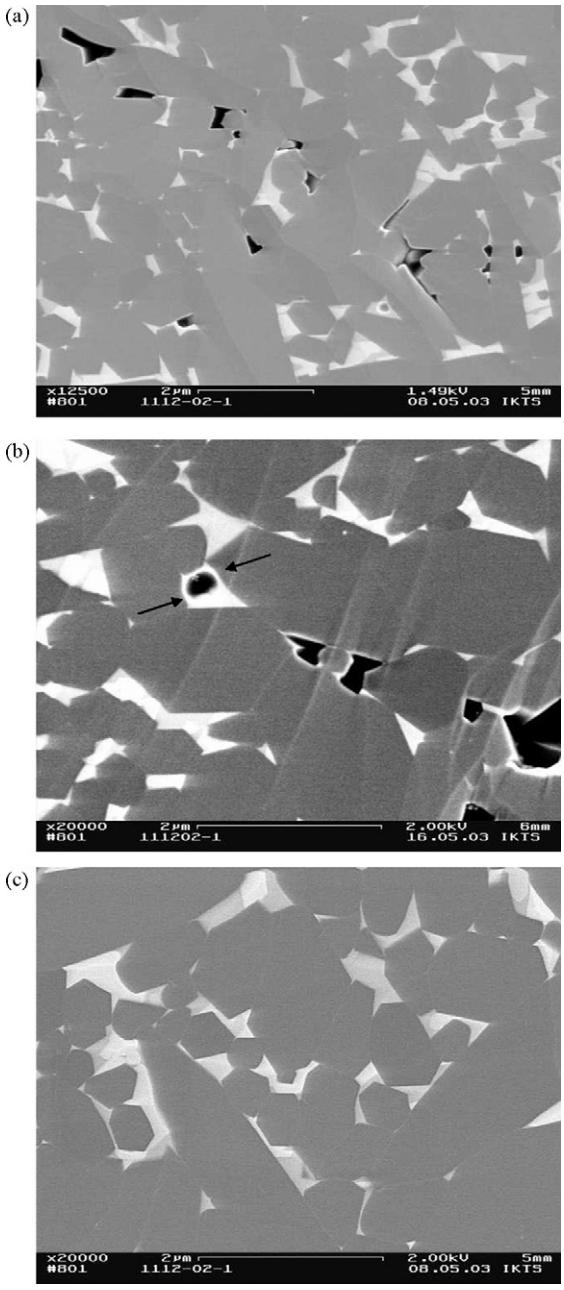

Fig. 6. FESEM micrographs of cross sections produced by ion beam cutting (sample 8Y2Al GPS).

of Si_3N_4.[19,20] Therefore, the internal tensile stresses in the grain boundary phase also decrease. Similar stress levels can occur due to crystallisation of the grain boundaries.[18,21–23,25] Recent investigations of oxynitride glasses showed that a formation of pores can take place during crystallisation of Y–Ca–Al–Si–O–N glasses.[25]

The stress relaxation in materials with Al_2O_3/Y_2O_3 or MgO additives is fast at temperatures above 1400–1500 °C due to the relative low viscosity of the grain boundaries. The relaxation stops near the glass transition temperature of the amorphous grain boundary phase at 800–1000 °C. The internal stresses can relax in different ways[25]:

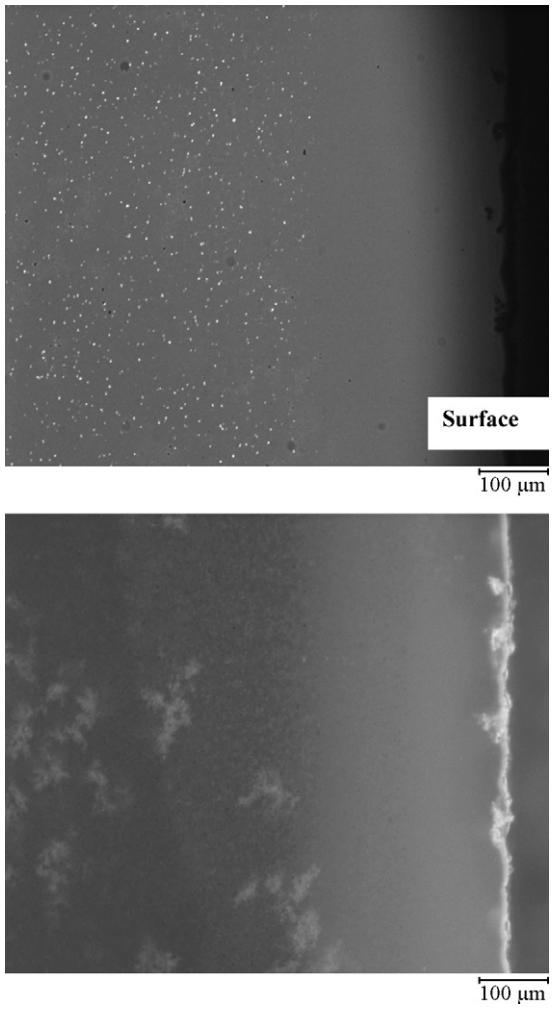

Fig. 7. Bright and dark field micrographs of the sample 6Y4AlGPS additionally heat treated at 1750 °C for 4 h at 1 bar N_2.

- Relaxation by solution, diffusion and precipitation mechanism: this mechanism was found for creep deformation. But these processes are quite slow and, therefore, this mechanism will not play a major role during cooling.
- Viscous flow of the grain boundary phase from the surface into the bulk. Model calculations[18] show that this mechanism is effective in the near surface area. This is also in agreement with the different structure of the "snow flakes" in the near surface area of the samples (Fig. 7).
- The main relaxation mechanism would be the formation of pores. As the formation of pores needs some activation energy, pores will only develop if the tensile stress is high enough.[24] If the nucleus of the pore is formed it will relax the stress by growing, i.e. emptying the neighbour triple junctions. This mechanism would explain why the empty triple junction exists as clusters alternating with the fully dense area. This formation mechanism explains also why the "snow flake" structure is so stable during sintering below the eutectic temperature.

The starting points of the formation of pores can be pores already existing in the material. Therefore, for porous materials

similar structures were not observed (direct relaxation by growing of the larger pores). Furthermore in areas which sinter not as fast as the main body, a stronger interaction with the atmosphere normally exists. This interaction predominantly results in a reduction of the SiO_2 in the grain boundary due to evaporation of SiO. This will increase the thermal expansion coefficient and crystallisation of the grain boundary. Therefore, the "snow flake" structures increasingly occur in these areas.

In the sinter-HIP method a pressure is still applied during cooling. This external isostatic pressure compensates the internal stresses.

Fig. 6c shows the microstructure under high resolution. In the grain boundary phase two phases are visible (different grey level) indicating the partial crystallisation of the grain boundary phase. This crystallisation results in segregation of the elements. The remaining glassy grain boundary phase consists of less Y_2O_3 than the crystalline phase. This changes the refractive index, as was mentioned by Keßler.[2] This can be an additional reason for "snow flakes", but was not verified here. The crystallisation of YAG in SiAlONs and LPS SiC takes place in very large crystals (several 10 μm) resulting in much higher segregations. On the other hand the formation of such large crystals will also localise the area in which pores can be formed.

5. Conclusions

The large scale optical inhomogeneities were analysed in different Si_3N_4 ceramics containing different additive ratios and densified by hot pressing, gas pressure sintering and spark plasma sintering.

In all analysed materials showing these optical inhomogeneities ("snow flakes") non-filled triple junctions were locally found which could be correlated with the "snow flake" structure. The most likely reason for this phenomenon is the internal tensile stress in the amorphous grain boundary phase. These stresses are caused by thermal mismatch between the grain boundary phase and the Si_3N_4 skeleton.

References

1. Petzow, G. and Herrmann, M., Silicon nitride ceramics. *Structure and Bonding*, *vol. 102*. Springer Verlag, Berlin, Heidelberg, 2002, pp. 47–167.
2. Keßler, S., Kristallisationsprozesse in heißgepresster Siliciumnitridkeramik. PhD thesis, Stuttgart, 1993.
3. Clarke, D. R., Large scale inhomogeneities in silicon nitride ceramics and its effect on oxidation. *Mat. Sci. Forum*, 1989, **47**, 110.
4. Lewis, H. M., SiAlONs and silicon nitrides; microstructural design and performance. *Mater. Res. Soc. Symp. Proc.*, 1993, **287**, 159–171.
5. Keßler, S., Schneider, D. and Herrmann, M., IKTS-Dresden, unpublished report.
6. Schilm, J., Herrmann, M. and Michael, G., Corrosion of YSiAlON- glasses in acidic and caustic media. *Sil. Ind.*, 2004, **69**, 317–324.
7. Höhn, S. and Obenaus, P., Ionenstrahlpräparation von keramischen Pulvern und Grünkörpern für die hochauflösende Rasterelektronenmikroskopie. *Sonderband der Praktischen Metallographie*, 2004, **36**, 200–303.
8. Private communication.
9. German, R. M., *Sintering theory and practice*. J Wiley & Sons Inc., N.Y., 1995.
10. Kleebe, H.-J., Structure and chemistry of interfaces in Si_3N_4 ceramics studied by transmission electron microscopy. *J. Ceram. Soc. Jpn.*, 1997, **105**, 453–475.
11. Herrmann, M., Schilm, J., Michael, G., Meinhardt, J. and Flegler, R., Corrosion of silicon nitride materials in acidic and basic solutions and under hydrothermal conditions. *J. Eur. Ceram. Soc.*, 2003, **23**, 585–594.
12. Herrmann, M., Boberski, C., Michael, G., Putzky, G. and Hermel, W., Redistribution of the liquid phase during sintering of silicon nitride. *J. Mater. Sci. Lett.*, 1993, **12**, 1641–1643.
13. Herrmann, M., Putzky, G., Siegel, S. and Hermel, W., *Einfluss von Zersetzungsreaktionen auf die Sinterung, cfi/Ber DKG*, *vol. 69*., 1992, pp. 375–382.
14. Can, A., Herrmann, M., McLachlan, D. S., Sigalas, I. and Adler, J., Densification of liquid phase sintered silicon carbide. *J. Eur. Ceram. Soc.*, 2006, **26**, 1707–1713.
15. Evans, A. G. and Clarke, D. R., In *Thermal stresses in severe environments*, ed. D. P. H. Hasselmann and R. A. Heller. Plenum Press, N.Y., 1980, pp. 629–648.
16. Peterson, I. M. and Tien, T.-Y., Effect of the grain boundary thermal expansion coefficient on the fracture toughness in silicon nitride. *J. Am. Ceram. Soc.*, 1995, **78**(9), 2345–2352.
17. Kreher, W. and Pompe, W., Stochastic internal stresses in heterogeneous materials. *Mater. Sci. Forum*, 1990, 62–64.
18. Keßler, H., *Innere Spannungen und Sekundärphasenkristallisation in flüssigphasengesinterten Keramiken, Dissertation, TU Darmstadt*., 1993.
19. Scholze, H., *Glass*. Springerverlag, NY, Berlin, 1991.
20. Herrmann, M., Schubert, Chr., Klemm, H. and Tangermann, K., Verfahren zur Herstellung eines Körpers aus einem Silicium enthaltenden nichtoxidischen Werkstoff und nach dem Verfahren hergestellter Körper, DE 197 12918, 1997.
21. Keßler, H., Kleebe, H. J., Cannon, R. W. and Pompe, W., Influence of internal stresses on crystallization of intergranular phases in ceramics. *Acta Metall. Mater.*, 1992, **40**(9), 2233–2245.
22. Keßler, H., Herrmann, M. and Pompe, W., The effect of transformation stresses on the devitrivication kinetics of a minory phase in liquid phase sintered ceramics. *Acta Metall. Mater.*, 1995, **43**, 2789–2796.
23. Bossemeyer, H. G., *Devitrifikationskinetik in Siliziumnitridhochtemperaturkeramiken*. DGM Informationsgesellschaft mbH, 1995.
24. Bahr, H. A., Balke, H., Pompe, W. and Werdin, S., Unsteady-state pore formation at grain boundaries. *Neue Huete*, 1989, **34**(6), 201–207.
25. Lichvár, P., Šajgalík, P., Liška, M. and Galusek, D., $CaO–SiO_2–Al_2O_3–Y_2O_3$ glasses as model grain boundary phases for Si_3N_4 ceramics. *J. Eur. Ceram. Soc.*, 2007, **27**, 429–436.